

In-situ Mössbauer spectroscopy with MIMOS II

Iris Fleischer · Göstar Klingelhöfer · Richard V. Morris ·
Christian Schröder · Daniel Rodionov ·
Paulo A. de Souza · the MIMOS II team

© Springer Science+Business Media B.V. 2011

Abstract The miniaturized Mössbauer spectrometer MIMOS II was developed for the exploration of planetary surfaces. Two MIMOS II instruments were successfully deployed on the martian surface as payload elements of the NASA Mars Exploration Rover (MER) mission and have returned data since landing in January 2004. Mössbauer spectroscopy has made significant contributions to the success of the MER mission, in particular identification of iron-bearing minerals formed through aqueous weathering processes. As a field-portable instrument and with backscattering geometry, MIMOS II provides an opportunity for non-destructive in-situ investigations for a range of applications. For example, the instrument has been used for analyses of archaeological artifacts, for air pollution studies and for in-field monitoring of green rust formation. A MER-type MIMOS II instrument is part of the payload of the Russian Phobos-Grunt mission, scheduled for launch in November 2011, with the aim of exploring the composition of the martian moon Phobos. An advanced version of the instrument, MIMOS IIA, that incorporates capability for elemental analyses, is currently under development.

I. Fleischer (✉) · G. Klingelhöfer · D. Rodionov
Institute of Inorganic and Analytical Chemistry, Johannes Gutenberg University of Mainz,
Mainz, Germany
e-mail: fleischi@uni-mainz.de

R. V. Morris
NASA Johnson Space Center, Houston, TX, USA

C. Schröder
University of Bayreuth and University of Tübingen, Tübingen, Germany

D. Rodionov
Space Research Institute IKI, Moscow, Russia

P. A. de Souza
Tasmanian ICT Centre, Hobart, Australia

Keywords Miniaturized Mössbauer spectrometer · MIMOS II · Mars Exploration Rover mission · In-situ Mössbauer spectroscopy · Non-destructive analysis

Abbreviations

MIMOS II	Miniaturized Mössbauer spectrometer
NASA	National Aeronautics and Space Administration
MER	Mars Exploration Rover
IDD	Instrument Deployment Device
MI	Microscopic Imager
RAT	Rock Abrasion Tool
APXS	Alpha Particle X-ray Spectrometer
npOx	Nanophase ferric oxide
XRD	X-Ray Diffraction
XRF	X-Ray Fluorescence
SDD	Silicon Drift Detector

1 Introduction

MIMOS II, the miniaturized Mössbauer spectrometer, was developed for the mineralogical exploration of solid planetary surfaces. The instrument consists of a sensor head measuring $50 \times 50 \times 90$ mm and an electronics board.

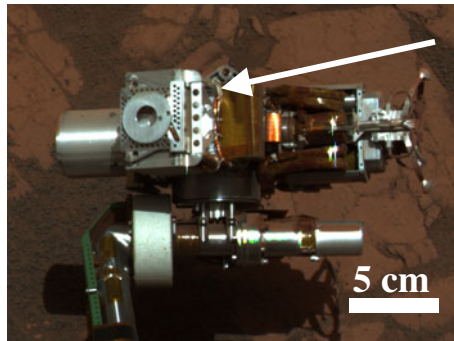
Two instruments have successfully been employed on the martian surface since January 2004 as payload elements of the two NASA Mars Exploration Rovers (MER) Spirit and Opportunity [1, 2]. On Mars, MIMOS II has proven its ability to work at temperatures as low as 200 K and at an atmospheric pressure of ~ 7 mbar. The backscattering instrument geometry does not require any sample preparation, which is a great advantage for measurements on the surface of another planet, and enables non-destructive analyses of terrestrial samples. As a field-portable instrument, MIMOS II has also been employed in a range of field studies. This paper provides a review of results from both extraterrestrial and terrestrial applications of MIMOS II instrumentation.

2 MER Mössbauer results

The twin Mars Exploration Rovers Spirit and Opportunity are equipped with a suite of analytical instruments, including a panoramic camera, a miniature thermal emission spectrometer and four contact instruments mounted on an Instrument Deployment Device (IDD), comprising a Microscopic Imager (MI), a Rock Abrasion Tool (RAT), an Alpha-Particle- X-ray spectrometer (APXS) and the miniaturized Mössbauer spectrometer MIMOS II. Figure 1 shows the instrument mounted on Opportunity's IDD, as imaged by the rover's panoramic camera.

The primary scientific objective of the MER mission was to search for traces of past water activity at two sites on the martian surface, Gusev crater and Meridiani Planum [2]. Whenever possible, observations of a surface target were carried out by several instruments, and evidence for aqueous alteration was found at both landing

Fig. 1 MIMOS II (arrow) on Opportunity's IDD. Image courtesy of NASA/JPL/Pancam



sites. Based on Mössbauer spectra obtained with MIMOS II, iron-bearing minerals were identified at both landing sites that are also known from terrestrial settings and form only under aqueous conditions.

Originally planned as a 90-sol mission (a sol is a martian day), Spirit's journey continued through March 2010, and Opportunity's investigations continue to the present day, more than seven years after landing. To date, ~ 150 Mössbauer spectra have been recorded on separate surface targets at each landing site. Because of diurnal temperature variations on Mars, spectra are stored in up to 13 separate temperature windows 10 K wide, covering the range from below 180 K to above 290 K.

2.1 Results from Gusev crater

Gusev crater was chosen as the landing site for MER Spirit because its morphology implies the former presence of a lake and lacustrine sediments [3]. During its 90-sol primary mission, however, Spirit traversed a basaltic plain. The first Mössbauer spectrum on the martian surface was obtained on soil and revealed its basaltic signature dominated by olivine and pyroxene. The rocks on the plain were found to be basaltic. In some cases, thin surface coatings containing iron oxides were observed to cover the rocks, thus providing evidence for at least a low degree of oxidation [4, 5]. An example spectrum is shown in Fig. 2a.

On sol 156, Spirit started investigating the Columbia Hills. Instead of the relatively fresh, olivine-rich rocks on the plains, the rover encountered pervasively weathered rocks [6, 7]. With MIMOS II, hematite ($\alpha\text{-Fe}_2\text{O}_3$) and goethite ($\alpha\text{-FeOOH}$) were detected in outcrop rocks [8]. An example spectrum is shown in Fig. 2b. Goethite also occurs in terrestrial settings, where it normally forms only under aqueous conditions. Its presence is thus evidence that the rocks of the Columbia Hills came into contact with water [7, 8]. The combination of data from MIMOS II and other MER instruments revealed the presence of carbonate assemblages that probably precipitated from carbonate-rich solutions under hydrothermal conditions [9].

On sol 744, after crossing the summit of Husband Hill, Spirit reached Home Plate, a circular, layered plateau in the inner basin of the Columbia Hills ~ 90 m in diameter and 2–3 m high that likely originated from a hydrovolcanic explosion and deposition of pyroclastic material [10]. MIMOS II Mössbauer spectra reveal that Home Plate rocks are rich in magnetite. At the west side, rocks contain significant amounts of

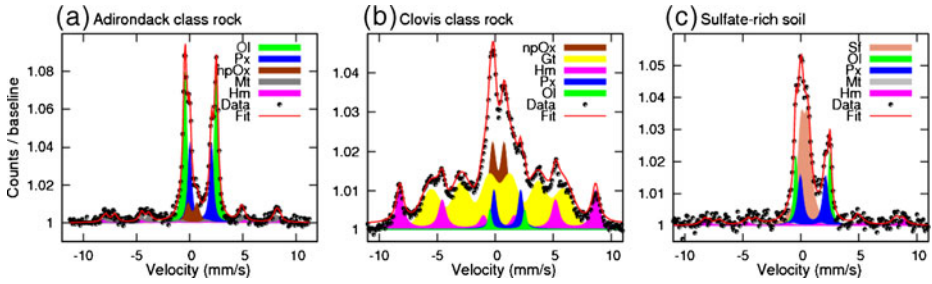


Fig. 2 Mössbauer spectra obtained at Gusev crater. **a** weakly-weathered Adirondack-class basaltic rock, **b** pervasively weathered Clovis class rock, **c** sulfate-rich soil. Legend: *Ol* olivine, *Px* pyroxene, *npOx* nanophase ferric oxide, *Mt* magnetite, *Hm* hematite, *Gt* goethite, *Sf* ferric sulfate

olivine and nanophase ferric oxide (npOx), while high abundances of pyroxene and little olivine are present at the east side [11]. This compositional transition may have originated from a combination of high and low temperature alteration processes [12].

Spirit spent its third martian winter on the northern slope of Home Plate and subsequently explored a small valley to the west. After a drive on sol 1871, the rover broke through a thin crust and became embedded in a deposit of mixed sulfate-rich and basaltic soil. An extensive investigation was initiated of freshly exposed, bright material. In agreement with high sulfur contents detected with the APXS, Mössbauer spectra revealed the presence of ferric sulfates (Fig. 2c). These, together with the nature of the crust, point to the occurrence of dissolution and precipitation processes just beneath the surface [13].

Communication with Spirit was lost at the onset of its fourth martian winter in March 2010. Attempts to re-establish communication were terminated in May 2011, officially completing Spirit's mission.

2.2 Results from Meridiani Planum

Opportunity's landing site at Meridiani Planum was chosen because hematite indicative for aqueous processes had been detected from orbit [14]. Opportunity landed in ~20 m diameter Eagle crater, where the rover investigated an exposure of bright sedimentary outcrop rocks in the wall of the crater. With Opportunity's Mössbauer spectrometer, jarosite ($(\text{K,Na})\text{Fe}_3^{3+}(\text{SO}_4)_2(\text{OH})_6$) and hematite were detected in the outcrop matrix. An example spectrum is shown in Fig. 3a. The presence of jarosite is clear evidence for past water activity under acidic conditions at Meridiani Planum [15]. Hematite was also found to be the main constituent of mm-sized spherules (Fig. 3b) that have formed as sedimentary concretions (the so-called blueberries) within the outcrop rock and are weathering out by eolian erosion [16–18]. The hematite in both outcrop and spherules is characterized by two populations whose Mössbauer parameters exhibit different temperature-dependent behaviors [19]. The presence of different hematite populations implies more than one hematite-forming process or episode [17, 20].

The soil at Meridiani Planum was found to be practically identical to the soil at Gusev crater. The similarity of soils from these two locations on opposite sides of the planet indicates that martian soil is a globally distributed component [21]. To

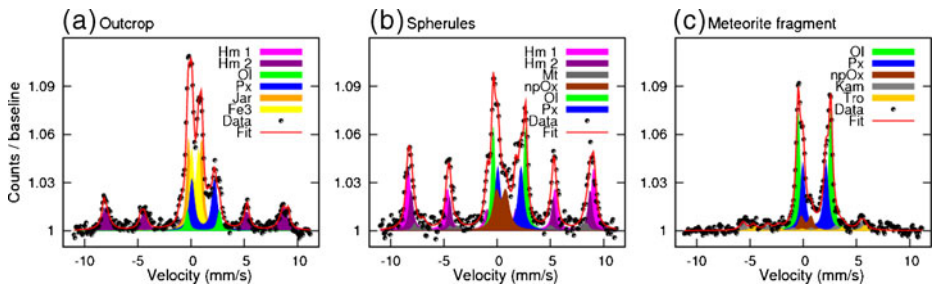


Fig. 3 Mössbauer spectra obtained at Meridiani Planum. **a** outcrop matrix, **b** hematite-rich spherules, **c** dark rock (meteorite fragment). Legend: *Hm* hematite, *Ol* olivine, *Px* pyroxene, *Jar* jarosite, *Fe3* unassigned ferric phase, *Mt* magnetite, *npOx* nanophase ferric oxide, *Kam* kamacite, *Tro* troilite

the present day, Opportunity has traversed more than 33 km. Along its traverse, the rover has investigated outcrop exposures on the plains and stratigraphic sections in the inner walls of a number of craters, the largest being Victoria with a diameter of ~ 800 m [22, 23]. For all investigated outcrop targets, the chemical and mineralogical compositions remain strikingly similar. Mössbauer spectra exhibit only minor variations, mostly with respect to the relative abundance of Fe-bearing phases [24]. Occasionally, Opportunity encountered dark rocks with no apparent connection to the ubiquitous bright outcrop. Typically, these rocks have dimensions of several centimeters and clusters are observed preferentially near craters. Based on their chemical and mineralogical composition derived from APXS and Mössbauer spectra, these “cobbles” can be distinguished into two groups interpreted as meteorite fragments and impact-breccias composed of local outcrop rock and basaltic sand [25, 26]. An example spectrum obtained on a meteorite fragment is shown in Fig. 3c. Opportunity also encountered six iron meteorites, whose weathering states provide information about the climate at Meridiani Planum since their impact [27–29].

Opportunity recently arrived at the rim of ~ 20 km diameter Endeavour crater, where the rover will investigate putative phyllosilicate-rich deposits that have been detected from orbit [30].

3 Mars analog studies

In support of the interpretation of the MER data set, terrestrial Mars analog sites were investigated. Recent field campaigns were focused on the investigation of sulfate- and oxide-rich mineral assemblages at Rio Tinto and Jaroso Ravine, Spain; two analog sites for Meridiani Planum [31, 32]. Studies were carried out with a combination of instruments, including MIMOS II, a Raman spectrometer [33] and the portable “Terra” XRD/XRF instrument [34].

The water of Rio Tinto exhibits a deep red color and a nearly constant acidic pH value of ~ 2.3 along its approximately 100 km long course. Sulfate minerals mainly form from aqueous alteration of the iron-rich sulfide minerals of the Iberian Pyrite Belt and precipitate from the river during dry, hot seasons [35]. Bedrock and evaporative precipitates were investigated in-situ at four different sampling sites

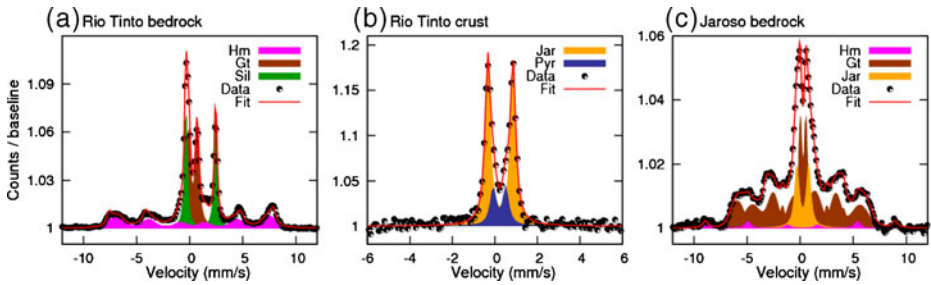


Fig. 4 Mössbauer spectra from Mars analog sites. **a** Rio Tinto river bedrock, **b** jarosite-bearing crust on Rio Tinto river bedrock, **c** assemblage of jarosite, goethite and hematite from Jaroso Ravine. Legend: *Hm* hematite, *Gt* goethite, *Sil* silicate, *Jar* jarosite, *Pyr* pyrite

during two field campaigns in 2008 and 2009. In addition to in-situ measurements, representative samples from all sampling sites were analyzed in detail after the field trip with laboratory instrumental setups.

The river bedrock was found to be constituted of conglomeratic, cemented materials with clast sizes in the range up to ~ 3 cm. The surface of the rocks is often covered with a dark crust, presumably from the influence of the acidic water. Mössbauer spectra reveal the presence of superparamagnetic goethite as the primary phase, with minor amounts of hematite and silicates from some clasts. An example spectrum is shown in Fig. 4 a. Portions of the river bedrock were covered with a red crust containing jarosite ($\text{KFe}_3(\text{SO}_4)_2(\text{OH})_6$) [31]. An example spectrum is shown in Fig. 4b.

Sulfate minerals generally precipitate close to the stream margin. Precipitates with popcorn-like texture a few centimeters in diameter are very common, usually colored white or yellow, sometimes mixed with small amounts of red or grey. From the combination of Mössbauer spectroscopy and XRD, ferric sulfates were detected in these samples, including ferricopiapite ($\text{Fe}_5^{3+}\text{O}(\text{SO}_4)_6\text{OH}\cdot 20\text{H}_2\text{O}$), coquimbite ($\text{Fe}_2(\text{SO}_4)_3\cdot 9\text{H}_2\text{O}$), and rhomboclase ($(\text{H}_5\text{O}_2)^+\text{Fe}^{3+}(\text{SO}_4)_2\cdot 2\text{H}_2\text{O}$). Crusts ~ 5 mm thick and several centimeters in diameter occur with a variety of colors including white and different shades of green and blue. They were found to contain the ferrous sulfates melanterite ($\text{Fe}^{2+}\text{SO}_4\cdot 7\text{H}_2\text{O}$) and rozenite ($\text{Fe}^{2+}\text{SO}_4\cdot 4\text{H}_2\text{O}$).

Jaroso Ravine, located within the Jaroso Hydrothermal System in south-eastern Spain, is the type locality of jarosite and a Mars analog site where mineral associations and formation processes can be studied in situ. With MIMOS II, jarosite was detected in association with goethite and hematite, in accordance with previous findings [36, 37]. An example spectrum is shown in Fig. 4c.

4 Terrestrial applications

As a field-portable instrument, MIMOS II has been employed in archaeological and environmental studies and in industrial applications. For the investigation of rare or precious materials such as archaeological artifacts, the backscattering geometry of MIMOS II enables non-destructive measurements.

On a Lekythos vase (500 B.C.), Mössbauer spectra were obtained on unpainted parts of the surface and on patterns painted with black and red color. The unpainted surface can be associated with poorly crystalline iron oxides, presumably produced during the firing process. Spectra obtained on black colored parts exhibit a sextet signature corresponding to well crystalline hematite. Spectra recorded on red colored parts were found to be practically identical to those from the unpainted surface, suggesting similar compositions [38].

In-situ analyses of ancient rock paintings were performed at Santana do Riacho, Minas Gerais, Brazil. For these measurements, MIMOS II was mounted on a tripod and put into contact with the painting on the wall. In total, six individual spots were investigated, which were separated by a few meters and exhibited distinctly different colors. The dominating Fe-oxide pigments were found to be hematite (red) and goethite (yellow/ochre), with an additional superparamagnetic Fe-oxide phase [39].

A sample of an ochre wall painting from a tomb in the district of Xunyi, Shaanxi, China, was investigated both at room temperature and at 200 K. Hematite and goethite were found to be present in the paint [40].

The investigation of ancient metallic artifacts yields information on their original composition, processing, and corrosion state. A Celtic helmet knob (discovered close to Aldrans, Tirol, Austria) was found to contain metallic iron, magnetite and superparamagnetic iron oxides. The higher concentration of magnetite on the surface compared to the interior suggests that magnetite stems from a corrosion process. The Mössbauer spectra, together with ashes and a patina on the artifact, indicate that the object may have been burnt as a sacrifice [41].

For another example, a roman mask and metallic fragments were found in excavations at “Villa von Allmend”, Saarland, Germany. Mössbauer spectra were obtained to determine whether a fragment was part of the mask or of another object. Significant amounts of wüstite (Fe_{1-x}O) were detected in the mask, along with magnetite, goethite and maghemite or hematite. The composition of the unidentified fragment was found to be clearly different: wüstite was not detected at all and magnetite, goethite, hematite and maghemite were identified with abundances different from those in the mask. Therefore, the fragment is not associated with the mask [41].

Air pollution studies were carried out in the metropolitan region of Vitória, Espírito Santo, Brazil. MIMOS II was installed in an airborne particle sampler. The accumulated particles were found to consist of hematite as the predominant phase, with goethite, pyrite, iron-bearing silicates, an ultrafine ferric phase and magnetite as subordinate phases. These minerals were found to originate from industrial plants producing iron-ore pellets (hematite), from handling and storing coal (pyrite), from steelwork plants (magnetite), from civil constructions (silicates), from industrial emissions and from strongly weathered tropical soils (ultrafine ferric phases). Hematite, goethite and silicates were also detected in soil [42].

A special experimental setup was developed for in-field monitoring of hydromorphic soils and the formation and transformation of the green-rust mineral fougèrite, $[\text{Fe}_{1-x}^{2+}\text{Mg}_y\text{Fe}_x^{3+}(\text{OH})_{2+2y}]^{x+}[\text{xA}, \text{mH}_2\text{O}]^{x-}$, where x is the ratio $\text{Fe}^{3+}/\text{Fe}_{\text{tot}}$ [e.g. 43]. Bore-hole investigations were carried out with MIMOS II placed inside a plexiglas tube. After programming instrument positions at several depths and acquisition intervals, the setup can work autonomously for several weeks [44]. Mössbauer spectra obtained during a field campaign in Fougères, France, are characteristic for fougèrite. Variations in the $\text{Fe}^{3+}/\text{Fe}_{\text{tot}}$ ratio were observed, providing evidence for fast redox transformations at well-defined points in the soil [43].

5 Conclusions and outlook

The miniaturized Mössbauer spectrometer MIMOS II has successfully been utilized in a wide range of extraterrestrial and terrestrial applications. Within the Mars Exploration Rover mission, two instruments contributed to the mission goal of searching for traces of past water activity by identifying minerals that are characteristic for aqueous weathering processes both at Gusev crater and at Meridiani Planum.

For MIMOS II as a field-portable instrument, a range of terrestrial applications has opened up. Investigations of rare and precious archaeological artifacts benefit from the possibility of performing non-destructive investigations. MIMOS II has been used to decipher the mineralogical composition of pigments used to paint pottery as well as on rock paintings. The original composition, corrosion state and treatment of metallic objects could be analyzed, and unassigned fragments could be compared to those objects based on their Mössbauer spectra. In autonomous, in-field setups, MIMOS II was successfully employed to trace sources of air pollution and to monitor transformations of the green-rust mineral fougérite.

A MER-type MIMOS II instrument is part of the payload of the Russian Phobos Grunt mission. Scheduled for launch in November 2011, the aim of this mission is to investigate the surface of the martian moon Phobos and return samples to Earth. Determining the surface mineralogical composition of Phobos will also shed light on the origin of the martian moons [45].

MIMOS IIA, an advanced version of the MIMOS II instrument, is equipped with a Silicon Drift Detector (SDD) system, which provides higher energy resolution that enables acquisition of X-ray fluorescence spectra suitable for elemental analysis in addition to Mössbauer spectra and will also decrease required integration times significantly [46]. A MIMOS IIA instrument was successfully tested during a field campaign at Mauna Kea, Hawaii [47], and it will surely open up new fields of application for in-situ Mössbauer spectroscopy.

Acknowledgements Development of the MIMOS II Mössbauer spectrometer was funded by the German Space Agency under contract 50QM99022 and supported by the Technical University of Darmstadt and the University of Mainz. C. Henrich is acknowledged for providing Fig. 4c. The support of the Russian space agency is acknowledged. We thank the reviewer of this manuscript for providing helpful comments.

References

1. Klingelhöfer, G., et al.: *J. Geophys. Res.* **108**(E12) 8067 (2003)
2. Squyres, S.W., et al.: *J. Geophys. Res.* **108**(E12), 8062 (2003)
3. Squyres, S.W., et al.: *Science* **305**, 794–799 (2004)
4. Morris, R.V., et al.: *Science* **305**, 833–836 (2004)
5. Haskin, L.A., et al.: *Nature* **436**, 66–69 (2005). doi:[10.1038/nature03640](https://doi.org/10.1038/nature03640)
6. Squyres, S.W., et al.: *J. Geophys. Res. Planet* **111**, E02S11 (2006)
7. Morris, R.V., et al.: *J. Geophys. Res. Planet* **111**, E02S13 (2006)
8. Klingelhöfer, G., et al.: *Hyperfine Interact.* **166**, 549–554 (2005)
9. Morris, R.V., et al.: *Science* **329**, 421–423 (2010)
10. Squyres, S.W., et al.: *Science* **316**, 738–742 (2007)
11. Schröder, C., et al.: *Lunar Planet. Sci.* **39**, 2153 (2008)
12. Schmidt, M.E., et al.: *Earth Planet. Sci. Lett.* **281**, 258–266 (2009)
13. Arvidson, R.E., et al.: *J. Geophys. Res. Planet* **115**, E00F03 (2010)
14. Christensen, P.R., et al.: *J. Geophys. Res.* **105**(E4), 9623–9642 (2000)

15. Klingelhöfer, G., et al.: *Science*, **306**, 1740–1745 (2004)
16. Morris, R.V., et al.: *Earth Planet. Sci. Lett.* **240**, 168–178 (2005)
17. McLennan, S., et al.: *Earth Planet. Sci. Lett.* **240**, 95–121 (2005)
18. Golden, D.C., et al.: *Am. Mineral.* **93**, 1201–1214 (2008)
19. Fleischer, I., et al.: *J. Geophys. Res. Planet* **115**, E00F06 (2010)
20. Morris, R.V., et al.: *Earth Planet. Sci. Lett.* **240**, 168–178 (2005)
21. Yen, A., et al.: *Nature* **436**, 49–54 (2005)
22. Squyres, S.W., et al.: *J. Geophys. Res. Planet* **111**, E12S12 (2006)
23. Squyres, S.W., et al.: *Science* **324**, 1058–1061 (2009)
24. Morris, R.V., et al.: *J. Geophys. Res. Planet* **111**, E12S15 (2006)
25. Fleischer, I., et al.: *J. Geophys. Res. Planet* **115**, E00F05 (2010)
26. Schröder, C., et al.: *J. Geophys. Res. Planet* **115**, E00F09 (2010)
27. Ashley, J.W., et al.: *J. Geophys. Res. Planet* **116**, E00F20 (2011)
28. Fleischer, I., et al.: *Meteorit. Planet Sci.* **46**(1), 21–34 (2011)
29. Schröder, C., et al.: *J. Geophys. Res. Planet* **113**, E06S22 (2008)
30. Wray, J.J., et al.: *Geophys. Res. Lett.* **36**, L21201 (2009)
31. Fleischer, I., et al.: *J. Phys.: Conf. Ser.* **217**, 012062 (2010)
32. Klingelhöfer, G., et al.: *Lunar Planet. Sci.* **41**, 2736 (2010)
33. Rull, F., et al.: *Lunar Planet. Sci.* **39**, 1616 (2008)
34. Blake, D., et al.: *Lunar Planet. Sci.* **40**, 1484 (2009)
35. Fernandez-Remolar, C., et al.: *Earth Planet Sci. Lett.* **240**, 149–167 (2005)
36. Rull, F., et al.: *EPSC Abs.* **5**, EPSC2010-845 (2010)
37. Martinez-Frias, J., et al.: *Earth Planets Space* **56**, v–viii (2004)
38. de Souza, P.A., et al.: *Hyperfine Interact.* **151/152**, 125–130 (2003)
39. Klingelhöfer, G., et al.: *Hyperfine Interact.* **C5**, 423–426 (2002)
40. Klingelhöfer, G., et al.: *Hyperfine Interact.* **144/145**, 371–379 (2002)
41. de Souza, P.A.: Dissertation, University of Mainz, Germany (2004)
42. de Souza, P.A., et al.: *J. Radioanal. Nucl. Chem.* **246**(1), 85–89 (2000)
43. Feder, F., et al.: *Geochim. Cosmochim. Acta* **69**, 4463–4483 (2005)
44. Rodionov, D., et al.: *Hyperfine Interact.* **167**(1) 869–873 (2006)
45. Rodionov, D., et al.: *Sol. Syst. Res.* **44**(5), 362–370 (2010)
46. Blumers, M., et al.: *Nucl. Instrum. Methods A* **624**(2), 277–281 (2010)
47. Klingelhöfer, G., et al.: *Lunar Planet. Sci.* **42**, 2810 (2011)